Sculpted-multilayer optical effects in two species of *Papilio* butterfly

Peter Vukusic, Roy Sambles, Christopher Lawrence, and Gavin Wakely

The wing-scale microstructures associated with two species of *Papilio* butterfly are described and characterized. Despite close similarities in their structures, they do not exhibit analogous optical effects. With *Papilio palinurus*, deep modulations in its multilayering create bicolor reflectivity with strong polarization effects, and this leads to additive color mixing in certain visual systems. In contrast to this, *Papilio ulysses* features shallow multilayer modulation that produces monocolor reflectivity without significant polarization effects. © 2001 Optical Society of America

OCIS codes: 000.1430, 310.6860, 330.1690, 260.5430, 230.4170.

1. Introduction

Multilayer structures are known to produce vivid iridescent coloration in certain butterflies.[1–3] The nature of these structures shows several variations on two central design themes.[4] The first, termed class I or *Morpho* type,[2] comprises layering within discrete ridged structures on the surface of scales that cover the wing. The second, referred to as class II or *Urania* type,[2] comprises continuous multilayering within the body of the iridescent scales.

One particular variation in class II multilayer design is brought about by modulations in the profile of the multilayering. These modulations, in orthogonal directions across the scale surface, have the effect of imposing concave structures into the scale. These concavities are characteristic of the iridescent scales of many gloss-*Papilio* butterflies and, in certain species, produce specific optical effects. Recent research[5] shows that the design of the multilayering in *Papilio palinurus* iridescent scales leads to bicolor production (with subsequent color stimulus synthesis[6] for human vision), retroreflection, and strong monocolor polarization conversion.

In this paper we present detailed evidence to account for the mechanism of coloration of *P. palinurus* and *P. ulysses* butterflies. Both species exhibit the concavity-variation of class II iridescent scales. Accordingly, despite their different coloration, one might expect them to employ the same mechanism for the production of analogous optical effects. We show here that this is not the case and that concavity depth and profile are the key factors responsible for this difference.

2. Experimental Procedures

Scanning and transmission electron microscopy are important techniques for analysis of scale surfaces, cross sections, and concavity profiles. For scanning electron microscopy a Hitachi Model S-3200N electron microscope was used, with samples first sputtered with 4 nm of gold. Transmission electron microscope (TEM) images were taken after fixing of samples in 3% glutaraldehyde at 21 °C for 2 h followed by rinsing in sodium cacodylate buffer. They were then fixed in 1% osmic acid in buffer for 1 h followed by block staining in 2% aqueous uranyl acetate for 1 h, dehydration through an acetone series (ending with 100% acetone), and embedding in Spurr resin. Postmicrotomed sample sections were stained with lead citrate and examined with a JEOL Model 100S TEM.

Reflection spectra from wing samples were collected with a Perkin-Elmer Model Lambda 900 UV/Vis/NIR spectrometer. Optical images of iridescent scales were taken through a Zeiss Jenalab polarizing microscope with a JVC Model TK-1280E color video camera.

(a)

(b)

Fig. 1. Full-color image of (a) *P. palinurus* and (b) *P. ulysses* butterflies showing their iridescent green and iridescent blue coloration [scale bars: (a) 1.5 cm and (b) 1.5 cm].

3. Results and Analysis

To the human observer, *P. palinurus*, and *P. ulysses* are distinct by their bright green and bright blue coloration, respectively (Fig. 1). The former exhibits a band of green iridescence across both fore and hind dorsal wings and the latter, bright blue across most of its fore and hind dorsal wings. Scanning electron microscope (SEM) images of the superficial layer of scales within these colored regions show their surfaces to consist of a fairly regular array of concavities

(Figs. 2 and 3). Ridging, a characteristic of the majority of lepidopteran wing scales, runs the full length of each scale with periodicity 4–6 μm and abruptly separates these depressions in one direction. Parallel to the ridging, the transition between concavities is less abrupt.

TEM images of the samples in cross section highlight the unique form of gloss-*Papilio* multilayering (Figs. 4 and 5). Sections taken through the concavities, perpendicular and parallel to the ridging, show the modulation in multilayering that causes the concavity profile.

Close inspection highlights three important features. First, in the scales of both species, the dimensions of each layer in the direction perpendicular to the local layer surface remain approximately constant regardless of position around a concavity. Second, the multilayer dimensions are smaller for the blue-colored *P. ulysses* than for the apparently green-colored *P. palinurus*. Finally, there is a distinct difference between the scales of the two species in the depths and the profiles of their concavities. In *P. palinurus*, the concavities are deeper and their sides are steeply inclined with respect to the plane to the scale. For *P. ulysses*, the scale concavities are shallower and their profiles effect much less-inclined side walls.

The optical effect of the different concavity profiles becomes evident in optical micrographs (Fig. 6). When illuminated and observed at near-normal incidence, the flat central regions in and between the concavities strongly reflect yellow in *P. palinurus* and blue in *P. ulysses*. Furthermore, in *P. palinurus*, the inclined sides of each concavity appear as blue annuli around the yellow concavity centers. The sides of the concavities in *P. ulysses* exhibit no analogous reflection.

It is interesting at this stage to ask two questions. First, for *P. palinurus*, why is normally incident light reflected back along the incident direction, as blue light, by the 45-deg-inclined sides of the concavities? Second, why is an equivalent effect not observed with the inclined sides of *P. ulysses* concavities even at near-UV wavelengths?

The key to answering these questions lies in appreciation of the contrast in concavity profiles between the two species. Whereas a substantial part of *P. palinurus* concavity sides are inclined at approximately 45 deg relative to the plane of the scale, the sides of *P. ulysses* concavities have inclinations of not more than 30 deg. Consequently, opposite sides of each *P. palinurus* concavity are perpendicular to each other, whereas in *P. ulysses* they are not. Notwithstanding actual multilayer dimensions, it is this that produces the fundamental differences in optical effects between the two species.

Clearly, for *P. palinurus*, single inclined sides of the concavities of the scales cannot reflect light back along the incident direction. In reality, each single side combines with the surface that is orthogonal to itself on the opposite side of the concavity. Retroreflection is effected in this way; i.e., normally incident
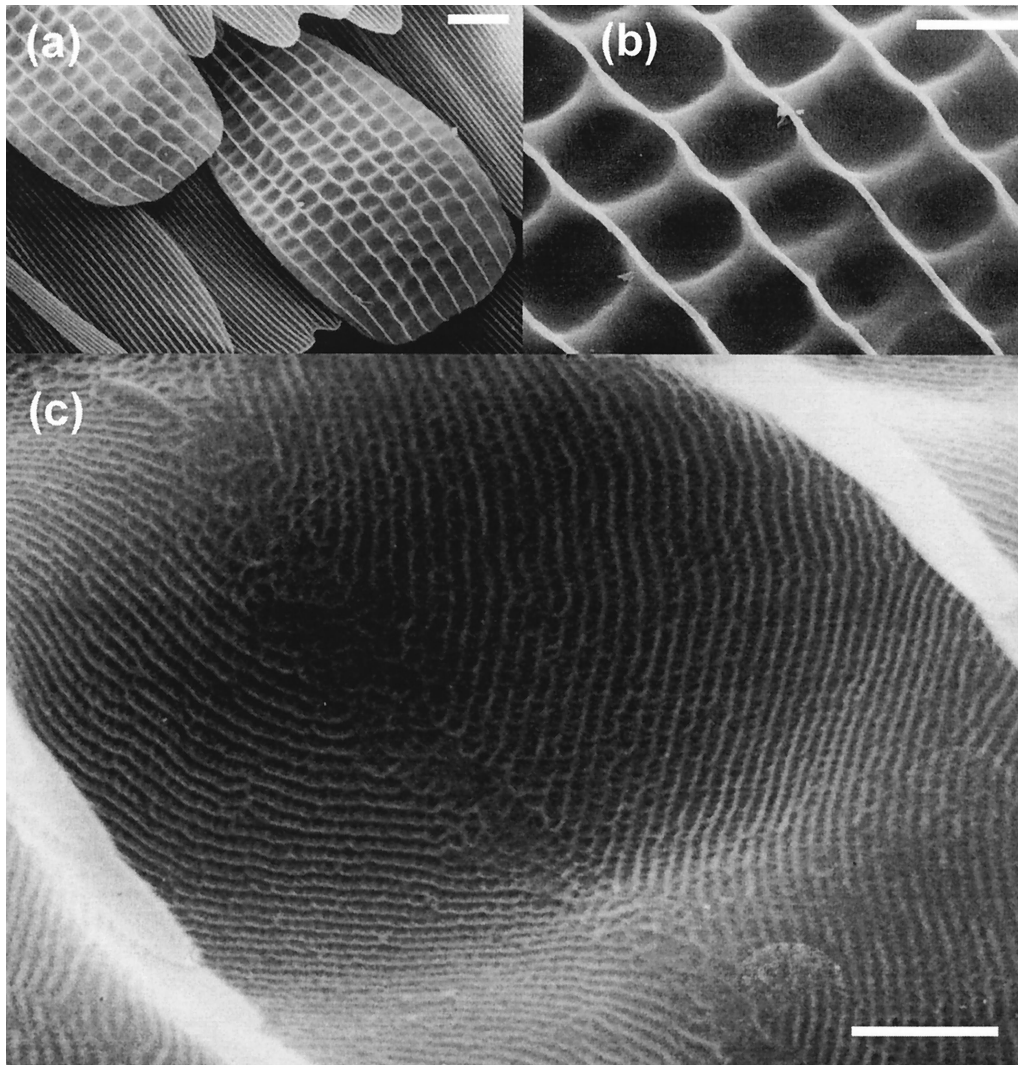
Fig. 2. SEM micrographs of *P. palinurus*: (a) whole iridescent scale on the wing, (b) a small region of iridescent scale, and (c) single concavity [scale bars: (a) 10 μm, (b) 5 μm, and (c) 1 μm].

blue light, reflected from one 45-deg-inclined surface, is directed across the concavity to the opposite orthogonal surface from where it returns parallel to the original incident direction. These pairs of inclined surfaces comprise near-identical multilayering and are both inclined at approximately 45 deg to the direction of normally incident light on the scale surface. Accordingly, their spectral reflectivity characteristics are closely matched. For *P. ulysses*, in which this surface orthogonality does not exist, such retroreflection is not possible.

Polarization conversion of blue light, through this double reflection, confirms this mechanism in *P. palinurus*. Upon crossing an input linear polarizer with an exit analyzer (while the sample is viewed with normally incident light), all yellow reflected light (reflected directly from the bottom of the concavities) is extinguished while a substantial portion of blue reflected light remains observable [Fig. 7(a)]. This necessarily implies that only the blue reflected light has undergone polarization conversion.

Such retroreflected polarization conversion is predicted from orthogonal surfaces only when the polarization vector of the incident light is at 45 deg to the plane of incidence. It does not occur when the incident polarization is perpendicular or parallel to the plane of incidence. Rotation of the wing scale, through 45 deg in the plane of the wing, changes the regions of the inclined sides of each concavity that exhibit this strong polarization conversion in the expected manner [Fig. 7(b)].

Optical theory can be used to predict reflectivity from a nonuniform system of flat multilayers.[7–9] The characteristic matrix of an assembly of n films may be calculated from the product of the matrices for the individual films taken in the correct order,

$$\begin{pmatrix} \mathbf{X} \\ \mathbf{Y} \end{pmatrix} = \left\{ \prod_{r=1}^{n} \begin{bmatrix} \cos \delta_r & \dfrac{i \sin \delta_r}{\eta_r} \\ i\eta_r \sin \delta_r & \cos \delta_r \end{bmatrix} \right\} \begin{pmatrix} 1 \\ \eta_{n+1} \end{pmatrix},$$
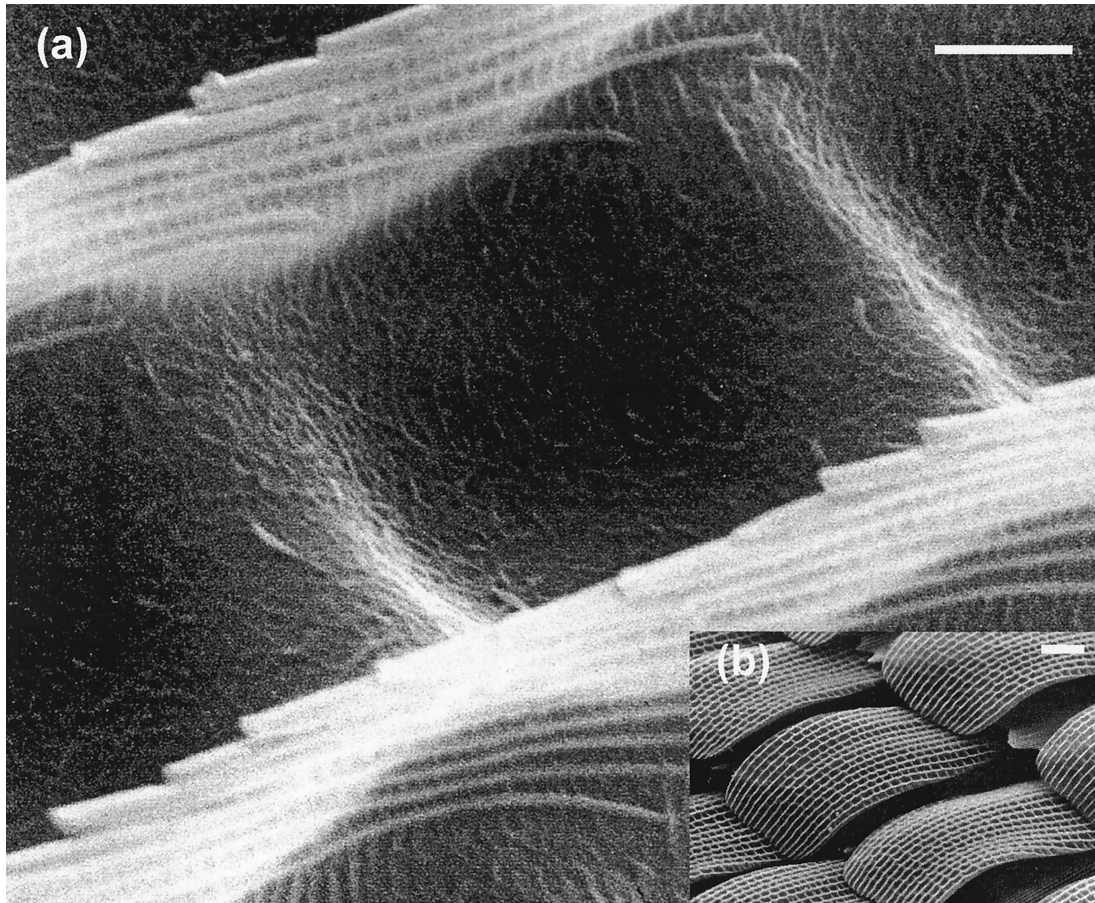
Fig. 3. SEM micrographs of *P. ulysses*: (a) single concavity and (b) iridescent scales on the wing [scale bars: (a) 1 μm and (b) 20 μm].

where $\eta_r = N_r \cos \theta_r$ and $\eta_{n+1} = N_{n+1} \cos \theta_{n+1}$ for TE waves; $\eta_r = N_r/(\cos \theta_r)$ and $\eta_{n+1} = N_{n+1}/(\cos \theta_{n+1})$ for TM waves; $\delta_r = (2\pi N_r d_r/\lambda)\cos \theta_r$; and $\mathbf{X}$ and $\mathbf{Y}$ correspond to $E_{i1} + E_{r1} + \eta_0(E_{i1} - E_{r1})$, respectively ($E_{i1}$ and E_{r1} are the incident and the reflected electric field vectors from the top surface of the system).

Here λ is the incident wavelength, d_r is the thickness of the rth film, N_r is the complex refractive index of the rth film (often written as $N = n - ik$, with n denoting the refractive index and k the extinction coefficient).

If θ_0 is the external angle of incidence, the values of the incident angle within a film, θ_r, may be calculated with Snell's Law. Once $\mathbf{X}$ and $\mathbf{Y}$ have been evaluated, the reflectance (R) of the assembly can readily be shown[9] to be

$$R = \frac{(\eta_0 X - Y)(\eta_0 X - Y)^*}{(\eta_0 X + Y)(\eta_0 X + Y)^*},$$

where * denotes complex conjugate.

Using this mathematical treatment, we produced a theoretical model of the reflectivity from the flat base and inclined sides of the *Papilio* concavities. We used published values[8,10,11] for cuticle complex refractive index and exact dimensions of individual layers obtained from direct measurement of TEM images of

P. palinurus and *P. ulysses* concavities [see Figs. 4(a) and 4(b), respectively]. (Although air and cuticle-layer dimensions are not constant down through each multilayer, they are generally in the range of 90–100 nm.)

For normal-incidence illumination and observation, strong yellow reflectance is predicted from the flat centers of *P. palinurus* concavities and blue reflectance for *P. ulysses*. This color difference between them, as expected, is caused by the difference in their layer dimensions. A double reflection, effected by two orthogonal 45-deg-inclined walls of *P. palinurus,* produces blue reflectivity of weaker intensity.

There is generally good agreement between the model predictions and the experimental data obtained with a reflection spectrometer (Fig. 8). In the experimental data and accompanying theoretical modeling, the multilayer systems of each species effect strong reflectance maxima, peaking at near 540 nm for *P. palinurus* and 460 nm for *P. ulysses*. Additionally, in both experiment and theory, we observe a secondary reflection maximum at 275 nm for *P. palinurus* and 250 nm for *P. ulysses* (Fig. 8 inset). These are artifacts of the multilayer systems present in both species and are too short in wavelength to be of biologic significance. They do, however, provide support for the theoretical model used in the analysis.
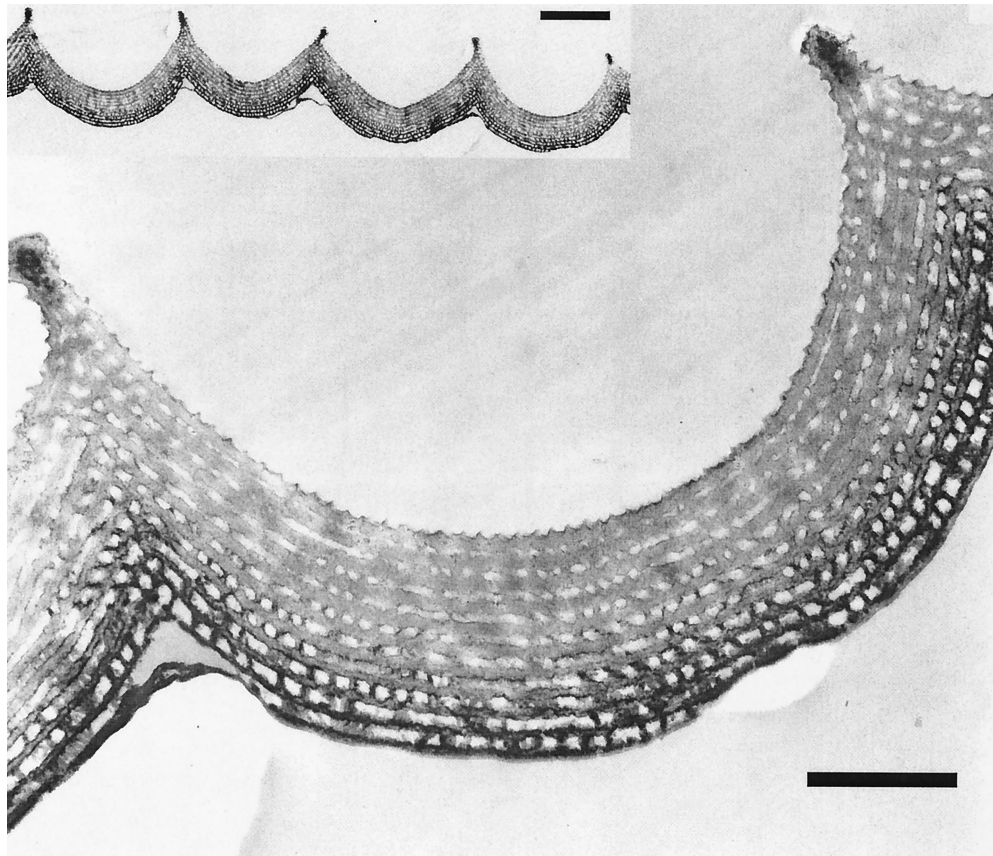
Fig. 4. TEM micrographs showing cross sections through iridescent scales of *P. palinurus* (perpendicular to ridges, with inset image showing the arrangement of several of the concavities across a single scale). [scale bars: 1 μm (inset 3 μm)].

However, it is worth making several additional points. The discrepancies in reflectivity levels between model and data, either side of the main peaks, are attributed to scatter from scale ridges and underlying noniridescent ground scales that cannot be accounted for in the modeling. Additionally, further discrepancy is brought about by uncertainty in dispersion of cuticle complex refractive index across the experimental wavelength range.

The TEM images of both species show evidence of strong differential staining (Figs. 4 and 5). This has previously been observed in TEM's of iridescent butterfly scales[12] but with less-extreme differential contrast. It is not considered to be an artifact of the preparation procedure: Therefore we should consider its significance. The purpose of block-and-section staining of the sample during the preparation process is well known.[13] Block staining with uranyl acetate renders fine structure visible by causing certain components to attract heavy metals ions and consequently scatter electrons differentially. Further staining with lead citrate, once the sample is in sectional form, enhances contrast between fine structure in the image. The dark contrast of the lower cuticle layers is indicative of the presence of different molecular species compared with the light-contrasted upper layers. We conjecture that this darker contrast is evidence of higher concentrations of melanin in the lower layers (melanin is the optically absorbing species present in the majority of butterfly scales[14]). High levels of melanin in the lower layers would increase optical absorption toward the bottom of the multilayer system while permitting strong reflectivity without absorption in the upper layers. This idea has been included in the theoretical modeling represented in Fig. 8. Within the model, the imaginary component of refractive index used to represent the optical absorption in the upper layers is less than that in the lower layers; this difference and their values are in line with measurements of k coefficients of single iridescent scales in other species[10] (i.e., for upper layers, $k = 0.06$ and for lower layers, $k = 0.25$, both at $\lambda = 550$ nm). Poorer fits between theory and data are produced if this differential absorbance model is not used.

Both species also exhibit some even finer surface texture across their iridescent scales. In *P. palinurus* this texture is in the form of a small zero-order grating of approximately 170-nm pitch and approximately 50-nm depth. It follows the surface profile in the area between the ridges running at 45 deg to the ridges. Similar surface texture is present in *P. ulysses* but in a much less-ordered arrangement. The dimensions of both these textures are believed to be too small to contribute any significant optical effects at visible and near UV. However, it is possible that
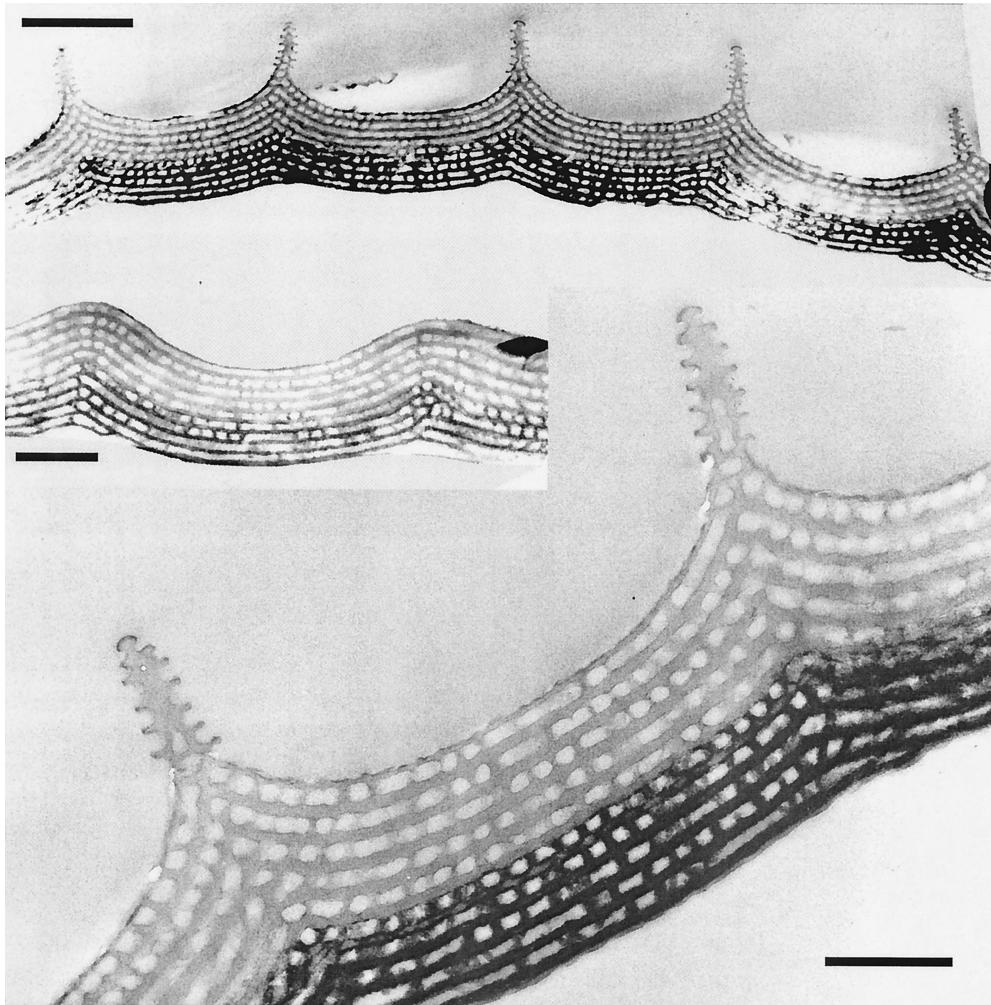
Fig. 5.   TEM micrographs showing cross sections through iridescent scales of *P. ulysses* (perpendicular to ridges, with bottom inset image showing cross section taken parallel to ridges and top inset image showing arrangement of several neighboring concavities). [scale bars: 1 μm (top inset 3 μm and bottom inset 1 μm)].

this provides some level of impedance matching, reducing broadband reflectivity from the topmost surface of the scale multilayer system.

It is generally believed that iridescent species exhibiting the continuous body-lamellae of class II scales do not posses ridge-lamellae associated with class I scales. Such lamellae, however, are evident in the ridges of *P. ulysses* (Fig. 9). One would assume that such complex structure would serve an optical purpose. Reflectivity calculations using layer dimensions suggest that the layered structure of the ridging is designed to reflect a wavelength band centered at approximately 380 nm. However, after we account for the limited number of layers and ridge occupancy, the maximum absolute level at which this band is reflected is less than 10%. This appears to make ridge-lamellae reflectivity insignificant in comparison with the reflectivity from the body-lamellae, even at 380 nm. The function, therefore, of the lamellar nature of the ridges on *P. ulysses* remains a puzzle.

When *P. palinurus* is illuminated with diffuse sunlight, green coloration can be observed in a limited region above its wings. Outside this perspective the wing coloration changes predictably; i.e., shorter wavelengths are reflected more strongly as observation angle approaches grazing incidence. It is for these conditions that the reflectivity characteristics of each orthogonal surface become mismatched, causing the retroreflective effect of each concavity to function less effectively. However, observation at increasingly nonnormal incidence is effected through large-angle reflections from the center and from single sides of each concavity.

P. ulysses visibility is more straightforward. It appears blue from directly above the wing; this is entirely due to single reflections from either the bottom or shallow sides of the concavities. Toward grazing incidence the wing color approaches deep violet, owing to larger angle reflections from the bottom and single sides of the shallow concavities.

4. Discussion

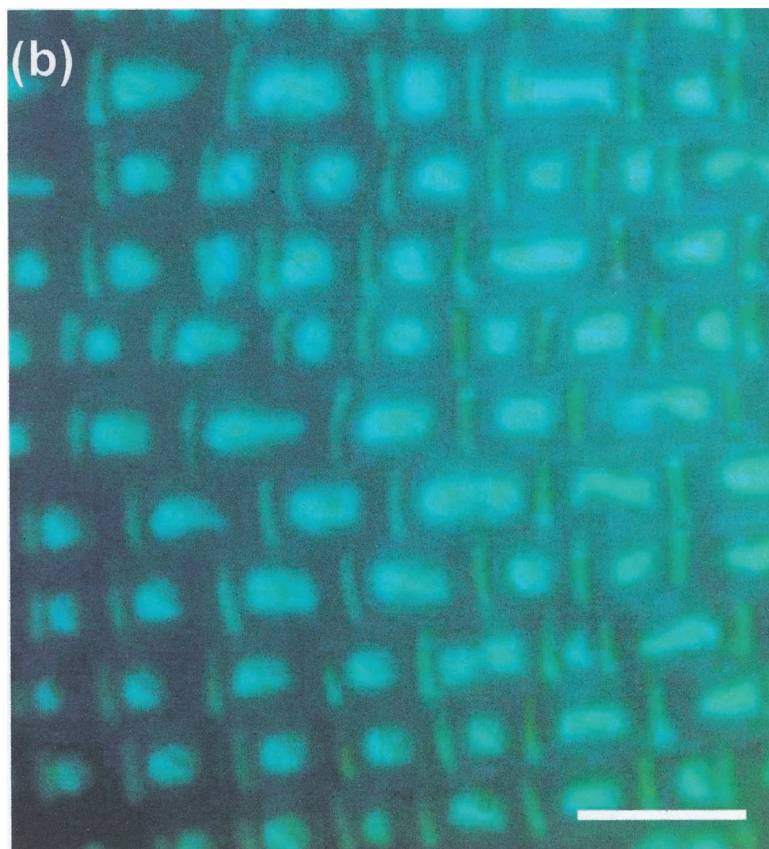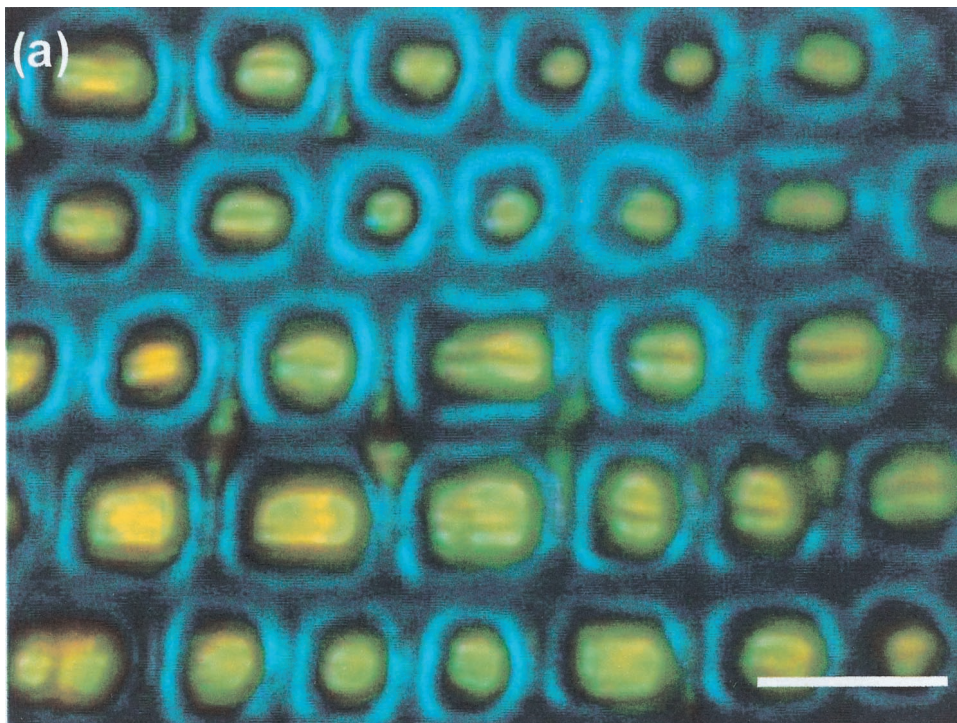Color stimulus synthesis[6] (CSS) is a phenomenon frequently found in nature, especially appearing in the

Fig. 6. Optical microscopy images of a region of (a) *P. palinurus* iridescent scale and (b) *P. ulysses* iridescent scale [scale bars: (a) and (b), 10 μm].

production of green colors. It is an effect whereby an additive mixture of two or more colors synthesizes the stimulus of a different color in the visual system of an observer.

In the animal kingdom, CSS of green is usually achieved through an additive mixture of structurally effected blue and pigmentary yellow[15] (or occasionally, both pigmentary blue and yellow[16]). The green
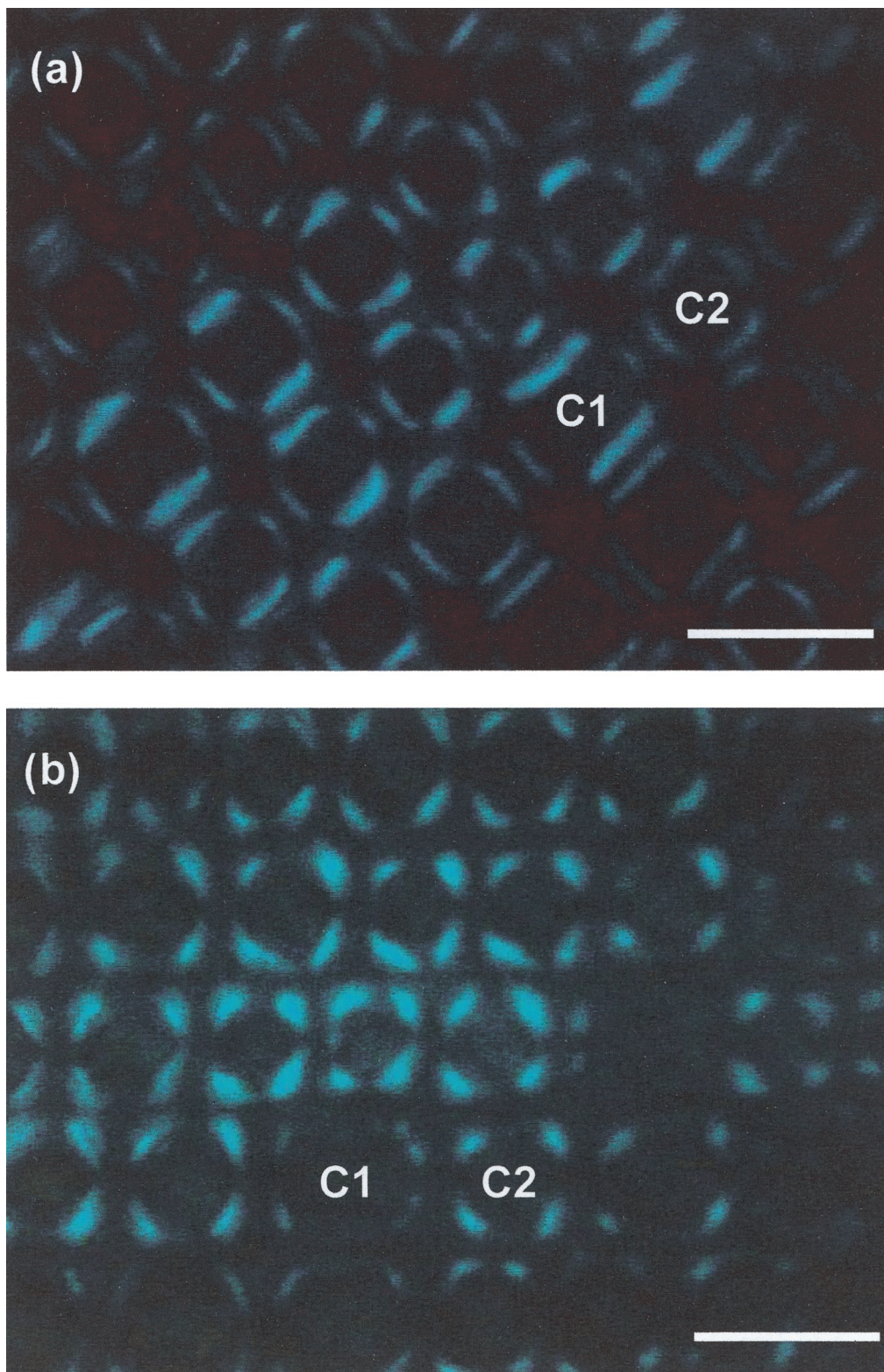
Fig. 7. Optical microscopy images of a region of a *P. palinurus* iridescent scale: (a) using input and output polarizers crossed with respect to each other and (b) input and output polarizers crossed with respect to each other but the sample rotated azimuthally through 45 deg from position in (a) [scale bars: (a) and (b), 10 μm]. C1 and C2 represent concavities 1 and 2 to clarify the sample rotation.

of many species of birds' feathers[17–20] and the integument of some amphibians[15,19,21] and reptiles[19] results from color mixing of yellow pigmentation with blue structural scattering effects. Purple, another synthesized color found in some feathers,[18,19] butterflies,[22] and in port-wine birthmarks,[23] is produced by the combination of red pigmentation with blue from structural scattering.
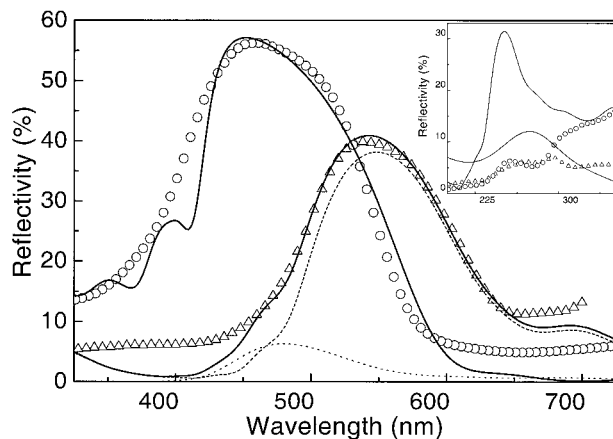
Fig. 8. Solid curves represent the results from the theoretical model and compare well with data collected from *P. palinurus* (triangles) and *P. ulysses* (circles). For *P. palinurus* the solid curve represents the integrated contribution of a single reflection from a flat *P. palinurus* multilayer (dashed curve) and a double reflection from an identical 45-deg-tilted multilayer (dotted curve). This shows the effect of the color mixing that produces the green of the wing. Inset graph shows secondary reflection maxima for theory and experiment for both butterflies at near-UV wavelengths that are not represented on the main graph.

In the wings of some butterflies, color stimulus may be synthesized in vision that is sensitive to both UV and visible wavelengths. Although to human vision, male *Eurema* butterflies appear characteristically yellow through pterin pigmentation, their scales offer an elaborate multilayer structure that reflects UV light strongly.[24] To conspecifics or predators, whose vision encompasses both spectral bands, the color of a male *Eurema* would appear as an additive mix of yellow and UV.

To normal human vision there is clearly CSS associated with the *P. palinurus* wing color. The green wing coloration is produced through the juxtaposition
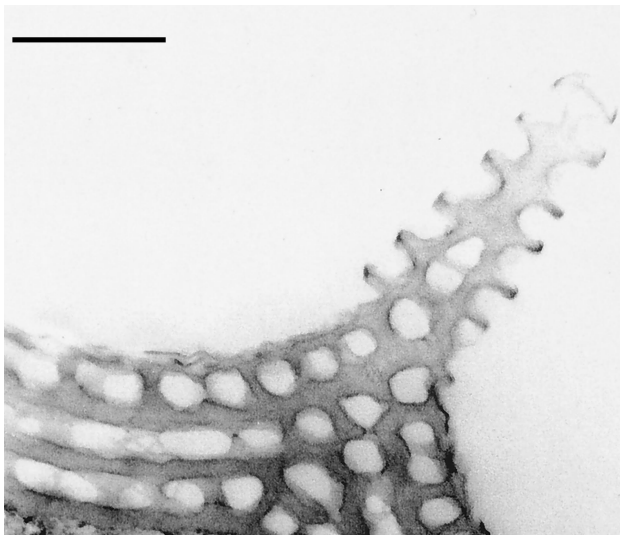

Fig. 9. High-magnification TEM micrograph of a cross section through a *P. ulysses* scale ridge (scale bar: 0.5 μm).

of yellow and blue concavity regions on each scale, these being too small to be individually resolved. This method of spatial-averaging CSS is the basis of modern color televisions, older systems of additive color photography and pointillistic painting.[14,25,26]

Blue and yellow, however, are classical complementary colors, and generally it is the addition of a color to its complementary that produces a colorless sensation, i.e., white.[27] Why then does the wing appear green?

The answer lies with the generalization made about complimentary colors: In reality, they will neutralize one another only when their respective luminances are suitably chosen.[28] In addition to this, both colors must be carefully defined for them to act as complementaries. Although it is common to refer to blue and yellow as complementaries, the colors blue and yellow encompass a range of wavelengths. Through the use of a standard chromaticity diagram[29] it can be demonstrated that green may be synthesized by additively mixing a specific blue to a specific yellow. It is in this way possible for *P. palinurus* to effect the stimulus of green from juxtaposed yellow and blue regions.

It is worth reflecting on the differences between the *P. palinurus* system that generates CSS with polarization effects and that of *P. ulysses* which, through a similar but shallower concavity profile, generates only one color and subsequently no CSS.

At normal incidence the base of the *P. ulysses* concavity reflects blue strongly. It accomplishes this through smaller multilayer dimensions than that of *P. palinurus*, which reflects yellow strongly. Were the *P. ulysses* concavities deeper (facilitating 45-deg-inclined side walls while maintaining the same multilayer dimensions), analogous retroreflection principles would apply to it as do to *P. palinurus*. This would lead to near-UV reflectivity by double reflection from the opposite sides of each concavity, retaining blue reflectivity from the flat concavity centers. In suitable visual systems this would effect CSS through additive mixture of the reflected blue and near UV. Furthermore, the UV component would show strong polarization conversion. The absence of this effect in *P. ulysses* compared with its presence in *P. palinurus* indicates that there are different predator, environmental, and conspecific selection pressures on each species.

The bright blue of the *P. ulysses* enhances long-range intraspecific communication in a similar way to the *Morpho* butterflies[9] of South America. In contrast, for *P. palinurus*, color stimulus of green from the blue and yellow reflected from its wing scales may offer camouflage against foliaceous backgrounds. Polarization sensitivity associated with blue-sensitive intraspecific photoreceptors (found in other papilios[30,31]) would enhance conspecific communication.

The charm of these butterflies is not just esthetic. The technique that *P. palinurus* employs to produce its coloration is, as far as we know, optically unique (although we have also identified similar but less-

pronounced effects in the related species of *P. crino*, *P. buddha*, and *P. blumei*). Through simple modulation in an otherwise uniform multilayer system, it displays high bicolor reflectivity that synthesizes a quite different color stimulus in certain visual systems. The structure shows strong local polarization conversion of one of the colors through a mechanism of orthogonal-surface retroreflection.[5] *P. ulysses*, through a shallower concavity profile, does not create this effect. It exhibits strong blue iridescence by virtue of appropriate layer dimensions in a 10–12 cuticle-layer system.

References

1. H. Ghiradella, "Light and color on the wing: structural colors in butterflies and moths," Appl. Opt. **30,** 3492–3500 (1991).
2. W. Lippert and K. Gentil, "Über lamellare Feinstrukturen bei den Schillerschuppen der Schmetterlinge vom Urania- und Morpho-typ," Z. Morphol. Oekol. Tiere **48,** 115–122 (1959).
3. T. F. Anderson and A. G. Richards, "An electron microscope study of some structural colors of insects," J. Appl. Phys. **13,** 748–758 (1942).
4. P. Vukusic, J. R. Sambles, and H. Ghiradella, "Optical classification of microstructure in butterfly wing scales," Photonics Sci. News **6,** 61–66 (2000).
5. P. Vukusic, J. R. Sambles, and C. R. Lawrence, "Structural colour: colour mixing in wing scales of a butterfly," Nature **404,** 457 (2000).
6. R. W. Burnham, R. M. Hanes, and C. J. Bartleson, *Color* (Wiley, New York, 1963).
7. A. Vašicek, *Optics of Thins Films* (North-Holland, Amsterdam, 1960).
8. M. F. Land, "The physics and biology of animal reflectors," Prog. Biophys. Mol. Biol. **24,** 75–106 (1972).
9. H. A. Macleod, *Thin-Film Optical Filters* (Adam Hilger, London, 1969).
10. P. Vukusic, J. R. Sambles, C. R. Lawrence, and R. J. Wootton, "Quantified interference and diffraction in single Morpho butterfly scales," Proc. R. Soc. London Ser. B **266,** 1403–1411 (1999).
11. M. Land, School of Biological Sciences, Sussex University, Brighton BN1 9QG, UK (personal communication, 1999).
12. J. Huxley, "The basis of structural colour variation in two species of Papilio," J. Entomol. Ser. A **50,** 9–22 (1975).
13. P. R. Lewis and D. P. Knight, *Staining Methods for Sectioned Material* (North-Holland, Oxford, 1977).
14. H. F. Nijhout, *The Development and Evolution of Butterfly Wing Patterns* (Smithsonian Institution, Washington, D.C., 1991).
15. D. L. Fox, *Animal Biochromes and Structural Colours* (University of California Press, Berkeley, Calif., 1976).
16. R. I. Vane-Wright, "The coloration, identification and phylogeny of Nessaea butterflies (Lepidoptera: Nymphalidae)," Bull. Br. Mus. (Nat. Hist.) Entomol. **38,** 2, 29–56 (1979).
17. R. Lewis, "The optics of feather colour," Biophotonics Int. (April, 1999), pp. 38–39.
18. C. W. Mason, "Structural colours in feathers I," J. Phys. Chem. **27,** 205–251 (1923).
19. H. M. Fox and G. Vevers, *The Nature of Animal Colours* (Sidgwick and Jackson, London, 1960).
20. F. Frank, "Die färbung der vogelfeder durch pigment und struktur," J. Orn. Lpz. **3,** 426–523 (1939).
21. C. E. Geldern von, "Color changes and structure of the skin of *Anolis carolinensis,*" Proc. Calif. Acad. Sci. **10,** 77–117 (1921).
22. R. I. Vane-Wright, Keeper of Entomology, Natural History Museum, London SW7 5BD, UK (personal communication, 1999).
23. J. Verne and F. Leyani, "Les dyschromies," Traité de dermatologie (Paris) **2,** 745–811 (1938).
24. H. Ghiradella, D. Aneshansley, T. Eisner, R. E. Silbergleid, and H. E. Hinton, "Ultra-violet reflection of a male butterfly: interference colour caused by thin layer elaboration of wing scales," Science **178,** 1214–1217 (1972).
25. R. M. Evans, "Visual processes and color photography," J. Opt. Soc. Am. **33,** 579–614 (1943).
26. D. L. MacAdam, "Perceptions of colour in projected and televised pictures," J. Soc. Motion Pict. Tel. Eng. **65,** 455–4669 (1956).
27. F. W. Billmeyer and M. Saltzman, *Principles of Color Technology* (Wiley, New York, 1981).
28. M. I. Sobel, *Light* (U. of Chicago Press, Chicago, 1987).
29. G. A. Agoston, *Color Theory and its Applications in Art and Design* (Springer-Verlag, New-York, 1987).
30. A. Kelber, "Why 'false' colours are seen by butterflies," Nature **402,** 251 (1999).
31. K. Bandai, K. Arikawa, and E. Eguchi, "Localisation of spectral receptors in the ommatidium of butterfly compound eye determined by polarisation sensitivity," J. Comp. Physiol. A **171,** 289–297 (1992).